Chapter 28
WFPC2 Data Analysis

In This Chapter...

Photometric Zero Point / 28-2
Photometric Corrections / 28-6
Polarimetry / 28-16
Astrometry / 28-18
Dithering / 28-19
Accuracy of WFPC2 Results / 28-23

This chapter deals with several topics pertaining to WFPC2 data analysis. We begin with a practical guide to photometry with WFPC2, in which we discuss how to accurately determine the zeropoint, photometric corrections that should be made to WFPC2 data, and common problems and their solutions. We start with the most important aspects of the photometric calibration that affect all observers, largely independently of the final accuracy desired, and in later sections consider subtle effects that can produce relatively small errors. A relatively simple calibration will produce photometric errors of 5 to 10%. With attention to more subtle effects, photometric accuracy between 2 and 5% can be achieved. We then discuss the analysis of polarization data, the astrometric characteristics of WFPC2 images, and the reconstruction of dithered data via the STSDAS package **dither**. Sub-pixel dithering is widely recognized—after the success of the Hubble Deep Field observations—as a valuable way to overcome in part the undersampling of WFPC2 images. Finally, we summarize various accuracies to be expected from well-calibrated WFPC2 observations.

Additional information on many WFPC2 data analysis topics can be found via the WFPC2 Clearinghouse. The Clearinghouse includes references to STScI documentation, publications from the astronomical literature, and user-submitted documentation, organized into more than 50 topics. The Clearinghouse can be found on the following web page:

`http://www.stsci.edu/ftp/instrument_news/WFPC2/Wfpc2_clear/wfpc2_clrhs.html`

28.1 Photometric Zero Point

The zero point of an instrument, by definition, is the magnitude of an object that produces one count (or data number, DN) per second. The magnitude of an arbitrary object producing DN counts in an observation of length EXPTIME is therefore:

$$m = -2.5 \times \log_{10}(\mathrm{DN} / \mathrm{EXPTIME}) + \mathrm{ZEROPOINT}$$

It is the setting of the zeropoint, then, which determines the connection between observed counts and a standard photometric system (such as Cousins RI), and in turn between counts and astrophysically interesting measurements such as the flux incident on the telescope.

Zero Points and Apertures

Each zero point refers to a count rate (DN/EXPTIME) measured in a specific way. The zeropoints published by Holtzman et al. (1995b) refer to counts measured in a standard aperture of 0.5" radius. The zeropoint derived from the PHOTFLAM header keyword, as well as in other STScI publications, refer—for historical continuity—to counts measured an “infinite” aperture. Since it is not practical to measure counts in a very large aperture, we use a nominal infinite aperture, defined as having 1.096 times the flux in an aperture with 0.5" radius. This definition is equivalent to setting the aperture correction between 0.5" radius and infinite aperture to exactly 0.10 mag.

28.1.1 Photometric Systems Used for WFPC2 Data

There are several photometric systems commonly used for WFPC2 data, often causing some confusion about the interpretation of the photometric zeropoint used—and of the photometry results themselves. Before continuing with the discussion of the photometry, it is worthwhile to define these photometric systems more precisely.

The first, fundamental difference between systems has to do with the filter set on which they are based. The WFPC2 filters do not have exact counterparts in the standard filter sets. For example, while F555W and F814W are reasonable approximations of Johnson V and Cousins I respectively, neither match is exact, and the differences can amount to 0.1 mag—clearly significant in precise photometric work. Other commonly used filters, such as F336W and F606W, have much poorer matches in the Johnson-Cousins system. We recommend that, whenever practical, WFPC2 photometric results be referred to a system based on its own filters. It is possible to define “photometric transformations” to convert these photometry results to one of the standard systems; see Holtzman et al. (1995b) for some examples. However, such transformations have limited precision, depend on the color range, metallicity, and surface gravity of the stars considered, and can easily errors of 0.2 mag or more, depending on the filter and on how much the spectral energy distribution differs from that of the objects on which the transformation is defined; this happens frequently for galaxies at high redshift.

Two photometric systems based on WFPC2 filters are the WFPC2 flight system, defined by the WFPC2 IDT and detailed in Holtzman et al. (1995b), and the synthetic system, also defined by the IDT and subsequently used in **synphot** as the VEGAMAG system. For more references, see Harris et al. (1993), Holtzman et al. (1995b), *WFPC2 ISR* 96-04, and the *Synphot User's Guide*.

The WFPC2 flight system is defined so that stars of color zero in the Johnson-Cousins UBVRI system have color zero between any pair of WFPC2 filters, and have the same magnitude in V and F555W. This system was established by Holtzman et al. (1995b) by observing two globular cluster fields, in ω Cen and in NGC 6752, with HST and from the ground; ground-based observations were taken both with WFPC2 flight-spare filters and with standard UBVRI filters. In practice, the system was defined by least-squares optimization of the transformation matrix. The stars near color zero which were observed are primarily white dwarfs, so the WFPC2 zeropoints defined in this system match the UBVRI zeropoints for stars with high surface gravity; the zeropoints for main sequence stars would be off by 0.02–0.05 mag, depending on the filter.

The zeropoints in the WFPC2 synthetic system, as defined in Holtzman et al. (1995b), are determined so that the magnitude of Vega, when observed through the appropriate WFPC2 filter, would be identical to the magnitude Vega has in the closest equivalent filter in the Johnson-Cousins system. For the filters in the photometric filter set, F336W, F439W, F555W, F675W, and F814W, these magnitudes are 0.02, 0.02, 0.03, 0.039, and 0.035, respectively. The calculations are done via synthetic photometry. In the **synphot** implementation, called the VEGAMAG system, the zeropoints are defined by the magnitude of Vega being *exactly* zero in all filters.

The above systems both tie the zeropoints to observed standards. In recent years, it has become increasingly common to use photometric systems in which the zeropoint is defined directly in terms of a reference flux in physical units. Such systems make the conversion of magnitudes to fluxes much simpler and cleaner, but have the side effect that any new determination of the absolute efficiency of the instrumental setup results in revised magnitudes. The choice between standard-based and flux-based systems is mostly a matter of personal preference.

The prevalent flux-based systems at UV and visible wavelengths are the AB system (Oke 1974) and the STMAG system. Both define an *equivalent flux density* for a source, corresponding to the flux density of a source of predefined spectral shape that would produce the observed count rate, and convert this equivalent flux to a magnitude. The conversion is chosen so that the magnitude in V corresponds roughly to that in the Johnson system. In the STMAG system, the flux density is expressed per unit *wavelength*, and the reference spectrum is flat in f_λ, while in the AB system, the flux density is expressed per unit *frequency*, and the reference spectrum is flat in f_ν. The definitions are:

$$m_{AB} = -48.60 - 2.5 \log f_\nu$$

$$m_{ST} = -21.10 - 2.5 \log f_\lambda$$

where f_ν is expressed in erg cm^{-2} s^{-1} Hz^{-1}, and f_λ in erg cm^{-2} s^{-1} Å^{-1}.

Another way to express these zero points is to say that an object with $f_\nu = 3.63\ 10^{-20}$ erg cm^{-2} s^{-1} Hz^{-1} will have m_{AB}=0 in every filter, and an object with $f_\lambda = 3.63\ 10^{-9}$ erg cm^{-2} s^{-1} Å^{-1} will have m_{ST}=0 in every filter. See also the discussion in the *Synphot User's Guide*.

28.1.2 Determining the Zero Point

There are several ways to determine the zero point, partly according to which photometric system is desired:

1. ***Do it yourself***: Over the operational life of WFPC2, a substantial amount of effort has gone into obtaining accurate zeropoints for all of the filters used on HST. Nonetheless, if good ground-based photometry is available for objects in your HST field, it can be used to determine a zeropoint for these observations. This approach may be particularly useful in converting magnitudes to a standard photometric system, provided all targets have similar spectral energy distribution; in this case the conversions are likely to be more reliable than those determined by Holtzman et al (1995b), which are only valid for stars within a limited range of color, metallicity, and surface gravity.

2. ***Use a summary list***: Lists of zeropoints have been published by Holtzman et al. (1995b), *WFPC2 ISR* 96-04, and *WFPC2 ISR* 97-10 (also reported in Table 28.1). The Holtzman et al. (1995b) zeropoints essentially *define* the WFPC2 flight photometric system; as discussed above, they are based on observations of ω Cen and NGC 6752 for the five main broad band colors (i.e., F336W, F439W, F555W, F675W, F814W), as well as synthetic photometry for most other filters. Transformations from the WFPC2 filter set to UBVRI are included, although these should be used with caution, as stated above. Holtzman et al. (1995b) also includes a cookbook section describing in detail how to do photometry with WFPC2. This paper is available from the STScI WWW or by sending e-mail to `help@stsci.edu`. The more recent compilations of zeropoints in *WFPC2 ISR* 96-04 and 97-10 use new WFPC2 observations, are based on the VEGAMAG system, and do not include new conversions to UBVRI.

3. ***Use the PHOTFLAM keyword in the header of your data***: The simplest way to determine the zeropoint of your data is to use the PHOTFLAM keyword in the header of your image. PHOTFLAM is the flux of a source with constant flux per unit wavelength (in erg s^{-1} cm^{-2} Å^{-1}) which produces a count rate of 1 DN per second. This keyword is generated by the synthetic photometry package **synphot**, which you may also find useful for a wide range of photometric and spectroscopic analyses. Using PHOTFLAM, it is easy to convert instrumental magnitude to flux density, and thus determine a magnitude in a flux-based system such as AB or STMAG (see previous Section); the actual steps required are detailed below.

Note that the zeropoints listed by Holtzman et al. (1995b) differ systematically by 0.85 mag from the **synphot** zeropoints in Table 28.1. Most of the difference, 0.75 mag, is due to the fact that the Holtzman zeropoints are given for gain 14, while the **synphot** zeropoints are reported for gain 7, which is generally used for science observations. An additional 0.1 mag is due to the aperture correction: the Holtzman zeropoint refers to an aperture of 0.5", while the **synphot** zeropoint refers to a *nominal* infinite aperture, defined as 0.10 mag brighter than the 0.5" aperture.

The tables used by the **synphot** package were updated in August 1995 and May 1997. With these updates, **synphot** now provides absolute photometric accuracy of 2% rms for broad-band and intermediate-width filters between F300W and F814W, and of about 5% in the UV. Narrow-band filters are calibrated using continuum sources, but checks on line sources indicate that their photometric accuracy is also determined to 5% or better (the limit appears to be in the quality of the ground-based spectrophotometry). Prior to the May 1997 update, some far UV and narrow-band filters were in error by 10% or more; more details are provided in *WFPC2 ISR* 97-10.

Table 28.1 lists the new values for PHOTFLAM. Please note that the headers of images processed before May 1997 contain out-of-date values of PHOTFLAM; the up-to-date values can be obtained by reprocessing the image, from the table, or more directly, by using the **bandpar** task in **synphot**—as long as the **synphot** version is up to date.[1] When using **bandpar**, it is also possible to incorporate the contamination correction (see “Contamination” on page 28-6) directly into the value of PHOTFLAM.

The **synphot** package can be used to determine the transformation between magnitudes in different filters, subject to the uncertainties related to how well the spectrum chosen to determine the transformation matches the spectrum of the actual source. The transformation is relatively simple using **synphot**, and the actual correction factors are small when converting from the WFPC2 photometric filter set to Johnson-Cousins magnitudes. For example, the following commands can be used to determine the difference in zeropoint between F814W filter and the Cousins I band for a K0III star on WF3 using the gain=7 setting:

```
sy> calcphot “band(wfpc2,3,a2d7,f814W)” crgridbz77$bz_54 stmag
```

where the Bruzual stellar atlas is being used to provide the spectrum for the K0 III star (`file = crgridbz77$bz_54`). The output is:

```
sy> calcphot “band(wfpc2,3,a2d7,f814W)” crgridbz77$bz_54 stmag
Mode = band(wfpc2,3,a2d7,f814W)
   Pivot       Equiv Gaussian
 Wavelength         FWHM
  7982.044        1507.155    band(wfpc2,3,a2d7,f814W)
Spectrum:  crgridbz77$bz_54
```

1. For instructions on how to retrieve STSDAS **synphot** tables, see “Getting the Synphot Database” on page A-15.

```
   VZERO            STMAG     Mode: band(wfpc2,3,a2d7,f814W)
      0.           -15.1045
```

Comparing this result with:

```
calcphot "band(cousins,I)" crgridbz77$bz_54 vegamag
Mode = band(cousins,I)
   Pivot     Equiv Gaussian
 Wavelength       FWHM
  7891.153      898.879     band(cousins,I)
 Spectrum: crgridbz77$bz_54
   VZERO        VEGAMAG     Mode: band(cousins,I)
     0.        -16.3327
```

shows that for a star of this color, the correction is 1.3 magnitudes (note that nearly all of this offset is due to the definition of STMAG; the F814W filter is a very close approximation to the Johnson-Cousins I, and color terms between these filters are very small). More details on the use of **synphot** can be found in the *Synphot User's Guide.*

28.2 Photometric Corrections

A number of corrections must be made to WFPC2 data to obtain the best possible photometry. Some of these, such as the corrections for UV throughput variability, are *time dependent*, and others, such as the correction for the geometric distortion of WFPC2 optics, are *position dependent*. Finally, some general corrections are needed as part of the analysis process, such as the aperture correction. We describe each class in turn.

28.2.1 Time-Dependent Corrections

The most important time-dependent correction is that for the contamination of the CCD windows, which affects primarily UV observations. Other time-dependent corrections are due to the change in operating temperature in April 1994 and to the variations of the PSF with focus position; the latter is also position-dependent (see "Aperture Correction" on page 28-13 for more information).

Contamination

Contaminants adhere to the cold CCD windows of the WFPC2. Although these typically have little effect upon the visible and near infrared performance of the cameras, the effect upon the UV is quite dramatic, and can reduce throughput by about 30% after 30 days for the F160BW filter. These contaminants are largely removed during periodic warmings of the camera and fortunately, in between these decontaminations, the effect upon photometry is both linear and stable, and can be removed using values regularly measured in the WFPC2 calibration program. Table 28.2 shows the contamination rates measured for each detector and Table 28.3 provides decontamination dates up until August 1997. Updated lists are kept on the WFPC2 WWW pages.

Table 28.1: Current Values of PHOTFLAM and Zeropoint in VEGAMAG system

Filter[a]	PC		WF2		WF3		WF4	
	New photflam	Vega ZP	New photflam	Vega ZP	New photflam	Vega ZP	New photflam	Vega ZP
F122M	8.088e-15	13.768	7.381e-15	13.868	8.204e-15	13.752	8.003e-15	13.778
F160BW	5.212e-15	14.985	4.563e-15	15.126	5.418e-15	14.946	5.133e-15	15.002
F170W	1.551e-15	16.335	1.398e-15	16.454	1.578e-15	16.313	1.531e-15	16.350
F185W	2.063e-15	16.025	1.872e-15	16.132	2.083e-15	16.014	2.036e-15	16.040
F218W	1.071e-15	16.557	9.887e-16	16.646	1.069e-15	16.558	1.059e-15	16.570
F255W	5.736e-16	17.019	5.414e-16	17.082	5.640e-16	17.037	5.681e-16	17.029
F300W	6.137e-17	19.406	5.891e-17	19.451	5.985e-17	19.433	6.097e-17	19.413
F336W	5.613e-17	19.429	5.445e-17	19.462	5.451e-17	19.460	5.590e-17	19.433
F343N	8.285e-15	13.990	8.052e-15	14.021	8.040e-15	14.023	8.255e-15	13.994
F375N	2.860e-15	15.204	2.796e-15	15.229	2.772e-15	15.238	2.855e-15	15.206
F380W	2.558e-17	20.939	2.508e-17	20.959	2.481e-17	20.972	2.558e-17	20.938
F390N	6.764e-16	17.503	6.630e-16	17.524	6.553e-16	17.537	6.759e-16	17.504
F410M	1.031e-16	19.635	1.013e-16	19.654	9.990e-17	19.669	1.031e-16	19.634
F437N	7.400e-16	17.266	7.276e-16	17.284	7.188e-16	17.297	7.416e-16	17.263
F439W	2.945e-17	20.884	2.895e-17	20.903	2.860e-17	20.916	2.951e-17	20.882
F450W	9.022e-18	21.987	8.856e-18	22.007	8.797e-18	22.016	9.053e-18	21.984
F467M	5.763e-17	19.985	5.660e-17	20.004	5.621e-17	20.012	5.786e-17	19.980
F469N	5.340e-16	17.547	5.244e-16	17.566	5.211e-16	17.573	5.362e-16	17.542
F487N	3.945e-16	17.356	3.871e-16	17.377	3.858e-16	17.380	3.964e-16	17.351
F502N	3.005e-16	17.965	2.947e-16	17.987	2.944e-16	17.988	3.022e-16	17.959
F547M	7.691e-18	21.662	7.502e-18	21.689	7.595e-18	21.676	7.747e-18	21.654
F555W	3.483e-18	22.545	3.396e-18	22.571	3.439e-18	22.561	3.507e-18	22.538
F569W	4.150e-18	22.241	4.040e-18	22.269	4.108e-18	22.253	4.181e-18	22.233
F588N	6.125e-17	19.172	5.949e-17	19.204	6.083e-17	19.179	6.175e-17	19.163
F606W	1.900e-18	22.887	1.842e-18	22.919	1.888e-18	22.896	1.914e-18	22.880
F622W	2.789e-18	22.363	2.700e-18	22.397	2.778e-18	22.368	2.811e-18	22.354
F631N	9.148e-17	18.514	8.848e-17	18.550	9.129e-17	18.516	9.223e-17	18.505
F656N	1.461e-16	17.564	1.410e-16	17.603	1.461e-16	17.564	1.473e-16	17.556
F658N	1.036e-16	18.115	9.992e-17	18.154	1.036e-16	18.115	1.044e-16	18.107
F673N	5.999e-17	18.753	5.785e-17	18.793	6.003e-17	18.753	6.043e-17	18.745
F675W	2.899e-18	22.042	2.797e-18	22.080	2.898e-18	22.042	2.919e-18	22.034
F702W	1.872e-18	22.428	1.809e-18	22.466	1.867e-18	22.431	1.883e-18	22.422
F785LP	4.727e-18	20.688	4.737e-18	20.692	4.492e-18	20.738	4.666e-18	20.701
F791W	2.960e-18	21.498	2.883e-18	21.529	2.913e-18	21.512	2.956e-18	21.498
F814W	2.508e-18	21.639	2.458e-18	21.665	2.449e-18	21.659	2.498e-18	21.641
F850LP	8.357e-18	19.943	8.533e-18	19.924	7.771e-18	20.018	8.194e-18	19.964
F953N	2.333e-16	16.076	2.448e-16	16.024	2.107e-16	16.186	2.268e-16	16.107
F1042M	1.985e-16	16.148	2.228e-16	16.024	1.683e-16	16.326	1.897e-16	16.197

a. Values are for the gain 7 setting. The PHOTFLAM values for gain 14 can be obtained by multiplying by the gain ratio: 1.987 (PC1), 2.003 (WF2), 2.006 (WF3), and 1.955 (WF4) (values from Holtzman et al. 1995b). For the zeropoints, add -2.5 log(gain ratio), or -0.745, -0.754, -0.756, and -0.728, respectively. The above values should be applied to the counts referenced to a nominal ‘‘infinite aperture’’, *defined* by an aperture correction of 0.10 mag with respect to the standard aperture with 0.5" radius.

Contamination is measured primarily from the bimonthly observations of the WFPC2 primary standard, the white dwarf GRW+70d5824; thus the contamination rates in Table 28.2 are directly applicable to blue objects. These observations have been supplemented, for the standard photometric filters, by observations of a stellar field in the globular cluster ω Cen (mean B–V ~ 0.7 mag); the contamination rates thus measured (in parentheses in Table 28.2) are generally in good agreement with those measured on GRW+70d5824. The ω Cen data also indicate a slightly higher contamination rate towards the center of each chip. For more details, see *WFPC2 ISR* 96-04. These results will be verified further with the analysis of UV observations of NGC 2100, a young globular cluster in the LMC.

The **synphot** package can be used to determine the effect of contamination on your observations. For example, the following command computes the expected countrate for a WF3, F218W observation taken 20 days (MJD=49835.0) after the April 8, 1995, decontamination, with the gain=7 setup:

```
sy> calcphot "wfpc2,3,f218w,a2d15,cont#49835.0" \
>>>  spec="bb(8000)" form=counts
```

Removing the `cont#49835.0` from the command will determine the countrate if no contamination was present. An 8000 K black body spectrum was chosen largely as a matter of simplicity—the correction values for contamination depend only on the filter chosen and do not reflect the source spectrum.

Table 28.2: Contamination Rates (Fractional Loss per Day)

Filter	PC1	+/-	WF2	+/-	WF3	+/-	WF4	+/-
F160BW	–0.263	0.030	–0.378	0.090	–0.393	0.051	0.381	0.066
F170W	–0.160	0.011	–0.284	0.005	–0.285	0.006	–0.232	0.006
F218W	–0.138	0.009	–0.226	0.015	–0.255	0.010	–0.213	0.033
F255W	–0.070	0.007	–0.136	0.017	–0.143	0.009	–0.108	0.042
F336W	–0.016 (–0.038)	0.008 (0.018)	(–0.043)	(0.010)	–0.057 (–0.046)	0.011 (0.008)	(–0.047)	(0.007)
F439W	–0.002 (0.002)	0.007 (0.014)	(–0.022)	(0.007)	–0.021 (–0.023)	0.010 (0.009)	(–0.023)	(0.007)
F555W	–0.014 (0.007)	0.006 (0.013)	(–0.007)	(0.007)	–0.016 (–0.009)	0.008 (0.009)	(–0.008)	(0.008)
F675W	–0.001 (–0.020)	0.006 (0.020)	(0.001)	(0.011)	–0.001 (0.002)	0.006 (0.011)	(0.004)	(0.011)
F814W	0.007 (0.013)	0.007 (0.019)	(–0.002)	(0.009)	0.003 (–0.000)	0.008 (0.009)	(–0.002)	0.016 (0.010)

Table 28.3: Dates of WFPC2 Decontaminations through August 1997[a]

Year.Day:Hour :Min	Day-Month-Year	Modified Julian Date	Year.Day:Hour: Min	Day-Month-Year	Modified Julian Date
1994.053:11:37	22-Feb-1994	49405.4840	1996.042:00:30	11-Feb-1996	50124.0208
1994.083:11:08	24-Mar-1994	49435.4639	1996.070:00:21	10-Mar-1996	50152.0147
1994.114:00:49	24-Apr-1994	49466.0340	1996.093:00:16	02-Apr-1996	50175.0111
1994.143:15:00	23-May-1994	49495.6250	1996.125:17:09	04-May-1996	50207.7146
1994.164:11:02	13-Jun-1994	49516.4597	1996.149:06:16	28-May-1996	50231.2614
1994.191:11:40	10-Jul-1994	49543.4861	1996.174:22:15	22-Jun-1996	50256.9277
1994.209:07:12	28-Jul-1994	49561.3000	1996.210:13:34	28-Jul-1996	50292.5653
1994.239:09:46	27-Aug-1994	49591.4069	1996.236:10:10	23-Aug-1996	50318.4242
1994.268:00:46	25-Sep-1994	49620.0319	1996.262:16:25	18-Sep-1996	50344.6840
1994.294:00:41	21-Oct-1994	49646.0285	1996.292:07:46	18-Oct-1996	50374.3236
1994.323:17:29	19-Nov-1994	49675.7285	1996.317:09:40	12-Nov-1996	50399.4031
1994.352:06:00	18-Dec-1994	49704.2500	1996.350:00:00	15-Dec-1996	50432.0417
1995.013:16:14	13-Jan-1995	49730.6764	1996.354:12:33	19-Dec-1996	50436.5229
1995.043:01:54	12-Feb-1995	49760.0792	1997.007:23:41	07-Jan-1997	50455.9875
1995.070:14:30	11-Mar-1995	49787.6042	1997.040:00:00	09-Feb-1997	50488.0006
1995.098:10:29	08-Apr-1995	49815.4368	1997.054:19:08	23-Feb-1997	50502.7978
1995.127:01:13	07-May-1995	49844.0507	1997.058:06:31	27-Feb-1997	50506.2721
1995.153:18:30	02-Jun-1995	49870.7708	1997.063:10:16	04-Mar-1997	50511.4278
1995.178:20:00	27-Jun-1995	49895.8333	1997.080:03:35	21-Mar-1997	50528.1494
1995.211:08:50	30-Jul-1995	49928.3681	1997.095:08:50	05-Apr-1997	50543.3681
1995.239:05:43	27-Aug-1995	49956.2382	1997.115:23:00	25-Apr-1997	50563.9583
1995.265:03:40	22-Sep-1995	49982.1528	1997.135:20:18	15-May-1997	50583.8460
1995.290:09:43	17-Oct-1995	50007.4053	1997.158:13:06	07-Jun-1997	50606.5461
1995.319:08:53	15-Nov-1995	50036.3706	1997.175:11:04	24-Jun-1997	50623.4612
1995.348:07:03	14-Dec-1995	50065.2929	1997.205:18:42	24-Jul-1997	50653.7795
1996.011:23:24	11-Jan-1996	50093.9750	1997.232:02:17	20-Aug-1997	50680.0952

a. The updated list of decontamination dates can be found on the World Wide Web at:
`http://www.stsci.edu/ftp/instrument_news/WFPC2/Wfpc2_memos/wfpc2_decon_dates.html`

Cool Down on April 23,1994

The temperature of the WFPC2 was lowered from –76 C to –88 C on April 23, 1994, in order to minimize the CTE problem. While this change increased the contamination rates (see above), it also improved the photometric throughput, especially in the UV, and greatly reduced the impact of warm pixels. Table 28.4 provides a partial list of corrections to Table 28.1 for the pre-cool down throughput. Including the MJD in a **synphot** calculation using up-to-date tables will automatically provide an estimate of PHOTFLAM corrected for this change.

Table 28.4: Ratio Between Pre- and Post-Cool Down Throughput

Filter	PC	PC (mag)	WF	WF (mag)
F160BW	0.865	–0.157	0.895	–0.120
F170W	0.910	–0.102	0.899	–0.116
F218W	0.931	–0.078	0.895	–0.120
F255W	0.920	–0.091	0.915	–0.096
F336W	0.969	–0.034	0.952	–0.053
F439W	0.923	–0.087	0.948	–0.058
F555W	0.943	–0.064	0.959	–0.045
F675W	0.976	–0.026	0.962	–0.042
F814W	0.996	–0.004	0.994	–0.007

PSF Variations

The point spread function (PSF) of the telescope varies with time, and these variations can affect photometry that relies on very small apertures and PSF fitting. Changes in focus are observed on an orbital timescale due to thermal *breathing* of the telescope and due to desorption, which causes a continual creeping of the focal position. This change has been about 0.7 μm per month until mid-1996, when it greatly slowed. Currently the focus drift is less than 0.3 μm per month. The effect of focus position on aperture photometry is described in *WFPC2 ISR* 97-01. About twice a year, the focal position of the telescope is moved by several microns to remove the effect of the desorption.

In addition, *jitter*, or pointing motion, can occasionally alter the effective PSF. The Observatory Monitoring System (OMS) files provide information on telescope jitter during observations (see Appendix C). These files are now regularly provided to the observer with the raw data. Observations taken after October 1994 have jitter files in the Archives. Limited requests for OMS files for observations prior to October 1994 can be handled by the STScI Help Desk (E-mail `help@stsci.edu`).

Recently, Remy et al. (1997) have been able to obtain high-quality photometry of well-exposed point sources by modeling the point spread function with TinyTim (Krist, 1995), and taking into account focus and jitter terms via a chi-squared minimization method. Similar results have been obtained using observed PSFs (Surdej et al., 1997), provided that the PSF used is less than 10" from the observed star and corresponds to a spectral energy distribution similar to that of the target. The WFPC2 PSF library was established to help users find suitable PSFs, if they exist, or carry out experiments with what is available. The PSF library is described in Wiggs et al. (1997) and can be found at the following URL:

`http://www.stsci.edu/ftp/instrument_news/WFPC2/Wfpc2_psf/wfpc2-psf-form.html`

28.2.2 Position-Dependent Corrections

In this Section we discuss the CTE correction and the possibly related long vs. short anomaly, the geometric distortion, the gain differences between different chips, and the effect of pixel centering.

Charge Transfer Efficiency

Shortly after launch it was discovered that WFPC2 had a substantial charge transfer efficiency (CTE) problem: objects appeared to be about 10% fainter when observed at the top of the chip (y~800) compared to when they were observed at the bottom of the chip (y~0). The April 23, 1994, cool down reduced the CTE problem to about a 4% effect peak-to-peak (Holtzman et al., 1995b) for a typical observation. The effect appears to be smaller, or nonexistent, in the presence of a moderate background.

Extensive observations made during Cycles 5 and 6 gave a much better characterization of the CTE calibration, indicating that its effect can be 5% or more (peak-to-peak) for faint images. *WFPC2 ISR* 97-08 quantifies the CTE effect under various observational circumstances and gives empirical rules to correct for it. After these corrections, the residual CTE effect for well-exposed stars is estimated to be less than 2%.

The correction depends on the average background, the average counts over the chip, and the counts in the source itself. Assuming a 2 pixel aperture, the corrected counts are given by:

$$counts_{corrected} = \left[1 + \frac{Y\text{-CTE}}{100} \times \frac{Y}{800} + \frac{X\text{-CTE}}{100} \times \frac{X}{800}\right] counts_{observed}$$

where X and Y are the coordinates of the star center in pixels, and *X-CTE* and *Y-CTE* are the percentile loss over 800 pixels in the x and y direction, respectively, given by:

$$Y\text{-}CTE = 10^{(0.7994 - 0.2564 \times \log_{10} BKG_{blank}) + (0.2478 - 0.0987 \log_{10} counts_{observed})}$$

and

$$X\text{-}CTE = 7.373 - 1.57 \times \log_{10}(counts_{observed})$$

Here, BKG_{blank} is the mean number of counts in DN for a blank region of the sky. For more details and other correction formulae, see *WFPC2 ISR* 97-08.

Long vs. Short Anomaly (non-linearity)

A comparison of repeated images of the same stellar field indicates that the count rates for the faint stars are higher for longer exposures. This apparent non-linearity appears to be a function of total counts in each source, rather than of count rates, and may depend on the image background. The magnitude errors produced appear to be less than 1% for well-exposed stars (over 30,000 e^-), but can rise to as much as 15% for faint stars (less than 300 e^-).[2] The effect is

2. See Casertano (1997), and Trauger (1997).

quantitatively similar to a loss of about 2 to 3 e^- per pixel in an aperture with a radius of 2 to 5 pixels. Although there is no evidence that this apparent non-linearity is, strictly speaking, position-dependent, it may be closely related to the CTE loss, and thus the two are often studied together.

An extensive program of observations is planned for Cycle 7 to characterize this non-linearity more completely. A preliminary report, based on data from Cycles 4 and 5, is available at:

`http://www.stsci.edu/ftp/instrument_news/WFPC2/Wfpc2_cte/ctetop.html`

Geometric Distortion

Geometric distortion near the edges of the chips results in a change of the surface area covered by each pixel. The flatfielding corrects for this distortion so that surface photometry is unaffected. However, integrated point-source photometry using a fixed aperture *will* be affected by 1 to 2% near the edges, with a maximum of about 4-5% in the corners. A correction image has been produced and is available from the Archive (`f1k1552bu.r9h`). The counts measured for a star centered at a given pixel position must be multiplied by the value of this image. A small residual effect, due to the fact that the aperture radius differs from the nominal size, depends on the aperture used and is generally well below 1%.

Gain Variation

The absolute sensitivities of the four chips differ somewhat. Flatfields have been determined using the gain=14 setup, normalized to 1.0 over the region [200:600,200:600]. However, most science observations are taken using the gain=7 setup. Because the gain ratio varies slightly from chip to chip, PHOTFLAM values will be affected. The count ratios for the different chips from Holtzman (1995b) are:

- ***PC1***: 1.987
- ***WF2***: 2.003
- ***WF3***: 2.006
- ***WF4***: 1.955

These count ratios should be included in the zeropoint calculation if using values from Holtzman et al. (1995b) on gain=7 data. Conversely, their reciprocals should be applied when using **synphot** zeropoints on gain=14 data. If you use the value of PHOTFLAM from the header to determine your zeropoint, the different gains for the different chips will already be included. Remember to use the new PHOTFLAM values provided in Table 28.1 or the post-May 1997 **synphot** tables; those included in the header for data taken before May 1997 will have less accurate values.

Pixel Centering

Small, sub-pixel variations in the quantum efficiency of the detector could affect the photometry. The position of star relative to the sub-pixel structure of the chip is estimated to have an effect of less than 1% on the photometry. At present there is no way to correct for this effect.

28.2.3 Other Photometric Corrections

Miscellaneous corrections that must be taken into account include: aperture corrections, color terms if transforming to non-WFPC2 filters, digitization noise and its impact on the estimate of the sky background, the effect of red leaks and charge traps, and the uncertainty of exposure times on short exposures taken with serial clocks on.

Aperture Correction

It is difficult to measure directly the total magnitude of a point source with the WFPC2 because of the extended wings of the PSF, scattered light, and the small pixel size. One would need to use an aperture far larger than is practical. A more accurate method is to measure the light within a smaller aperture and then apply an offset to determine the total magnitude. Typically, magnitudes will be measured in a small aperture well-suited to the data at hand—a radius of 2–4 pixels, with a background annulus of 10–15 pixels, has been found adequate for data without excessive crowding—and the results corrected to the aperture for which the zeropoint is known. The aperture correction can often be determined from the data themselves, by selecting a few well-exposed, isolated stars. If such are not available, encircled energies and aperture corrections have been tabulated by Holtzman et al. (1995a). If PSF fitting is used, then the aperture correction can be evaluated directly on the PSF profile used for the fitting.

For very small apertures (1–2 pixels), the aperture correction can be influenced by the HST focus position at the time of the observation. The secondary mirror of HST is known to drift secularly towards the primary and to move slightly on time scales of order of an orbit. The secular shift is corrected by biannual moves of the secondary mirror, but the net consequence of this motion is that WFPC2 can be out of focus by up to 3–4 μm of secondary mirror displacement at the time of any given observation. This condition affects the encircled energy at very small radii, and thus the aperture corrections, by up to 10% in flux (for 1 pixel aperture in the PC); see *WFPC2 ISR* 97-01 for more details. If the use of very small apertures is required—because of crowding, S/N requirements, or other reasons—users are strongly advised to determine the aperture correction from suitable stars in their images. If such are not available, an *approximate* aperture-focus correction can be obtained as described in *WFPC2 ISR* 97-01.

A standard aperture radius of 0."5 has been adopted by Holtzman et al. (1995b) (note that Holtzman et al. 1995a used a radius of 1."0). For historic consistency, the WFPC2 group at STScI and the **synphot** tasks in STSDAS refer all measurements to the total flux in a hypothetical infinite aperture. In order to avoid uncertain correction to such apertures, both in calibration and in science data, this infinite aperture is *defined* by an aperture correction of exactly 0.10 mag with respect to the standard 0."5 aperture. Equivalently, the *total* flux is defined as 1.096 times the flux in the standard aperture of 0."5 radius. In practice, this means that observers wishing to use our tables or the **synphot** zero points should:

1. Correct the measured flux to a 0."5 radius aperture.
2. Apply an additional aperture correction of –0.10 mag (equivalently, multiply the flux by 1.096).

3. Determine the magnitude using the zeropoints given.

See also the example in “An Example of Photometry with WFPC2” on page 28-15.

Color Terms

In some cases it may be necessary to transform from the WFPC2 filter set to more conventional filters (e.g., Johnson UBV or Cousins RI) in order to make comparisons with other datasets. The accuracy of these transformations is determined by how closely the WFPC2 filter matches the conventional filter and by how closely the spectral type (e.g., color, metallicity, surface gravity) of the object matches the spectral type of the calibration observations. Accuracies of 1–2% are typical for many cases, but much larger uncertainties are possible for certain filters (e.g., F336W with a red leak, see below), and for certain spectral types (e.g., very blue stars). Transformations can be determined by using **synphot**, or by using the transformation coefficients in Holtzman et al. (1995b).

Digitization Noise

The minimum gain of the WFPC2 CCDs, 7 e^-/ADU, is larger than the read noise of the chip. As a result, digitization can be a source of noise in WFPC2 images. This effect is particularly pernicious when attempting to determine sky values, because the measured values tend to cluster about a few integral values (dark subtraction and flatfielding cause the values to differ by slightly non-integral amounts). As a result, using a median filter to remove objects that fall within the background annulus in crowded fields, can cause a substantial systematic error, whose magnitude will depend on the annulus being measured. It is generally safer to use the mean, though care must then be taken to remove objects in the background annulus.

A more subtle effect is that some statistics programs assume Gaussian noise characteristics when computing properties such as the median and mode. Quantized noise can have surprising effects on these programs. The recommended strategies for sky determination are described in *WFPC2 ISR* 96-03.

Red Leaks

Several of the UV filters have substantial red leaks that can affect the photometry. For example, the U filter (F336W) has a transmission at 7500 Å that is only about a factor of 100 less than at the peak transmission at about 3500 Å. The increased sensitivity of the CCDs in the red, coupled with the fact that most sources are brighter in the red, makes this an important problem in many cases. The **synphot** tasks can be used to estimate this effect for any given source spectrum.

Charge Traps

There are about 30 macroscopic charge transfer traps, where as little as 20% of the electrons are transferred during each time step during the readout. These defects result in *bad pixels*, or in the worst cases, *bad columns* and should not be confused with microscopic charge traps which are believed to be the cause of the CTE problem. The traps result in dark tails just above the bad pixel, and bright tails for objects farther above the bad pixel that get clocked out through the defect during the readout. The tails can cause large errors in photometric and astrometric

measurements. In a random field, about 1 out of 100 stars are likely to be affected. Using a program which interpolates over bad pixels or columns (e.g., **wfixup** or **fixpix**) to make a cosmetically better image can result in very large (e.g., tenths of magnitude) errors in the photometry in these rare cases. See also “Charge Traps” on page 26-22.

Exposure Times: Serial Clocks

The serial clocks option (i.e., the optional parameter CLOCKS = YES in the Phase II proposal instructions) is occasionally useful when an extremely bright star is in the field of view, in order to minimize the effects of bleeding. However, when using this option, the shutter open time can have errors of up to 0.25 second. The error in the exposure time occurs as a result of the manner in which the shutters are opened when CLOCKS=YES is specified. Header information can be used to correct this error. If the keyword SERIALS = ON is in the image header, then the serial clocks were employed. The error in the exposure time depends on the SHUTTER keyword. If the value of this keyword is “A”, then the true exposure time is 0.125 second less than that given in the header. If instead the value is “B”, then the true exposure time is 0.25 second less than the header value.

Users should also note that exposure times of non-integral lengths in seconds cannot be performed with the serial clocks on. Therefore, if a non-integral exposure time is specified in the proposal, it will be rounded to the nearest second. The header keywords will properly reflect this rounding, although the actual exposure time will still be short as discussed above.

28.2.4 An Example of Photometry with WFPC2

This example shows the steps involved in measuring the magnitude of the star #1461 (Harris et al., 1993) in the Cousins I passband. The image used for this example can be obtained from the HST Archive, or from the WWW at:

`http://www.stsci.edu/ftp/instrument_news/WFPC2/Wfpc2_phot`

This WWW directory contains the materials for *WFPC2 ISR* 95-04, *A Demonstration Analysis Script for Performing Aperture Photometry*. Table 28.5 shows the results from an analysis script similar to *WFPC2 ISR* 95-04, but including some of the corrections discussed above.

```
Images: u2g40o09t.c0h[1] and u2g40o0at.c0h[1]
Position: (315.37,191.16)
Filter: F814W
Exposure Time: 14 seconds
Date of observation: MJD - 49763.4
```

Table 28.5: Magnitude of Star #1461 in ω Cen

Value	Description
2113.49 counts	Raw counts in 0.5" radius aperture (11 pixels for PC)
–48.63 = 2064.86 counts	Background subtraction (0.12779 counts x 380.522 pix obtained from a 40-pixel radius aperture with an annulus of 5 pixels)
x 0.9915 = 2047.31 counts	Correction for geometric distortion. Not needed if doing surface photometry.
=> 15.481 mag	Raw magnitude (=-2.5 x $\log_{10}$(2047.31 / 14 sec) + 20.894) NOTE: -2.5 x $\log_{10}$(1.987) has been added to the zeropoint from Table 28.1 (i.e., 21.639), since these calibrations were taken using the gain=14 setup. Most science observations use gain=7.
–0.10 = 15.381 mag	Aperture correction estimated from Holtzman (1995a).
–0.028 = 15.353 mag	CTE correction (using formulas 1, 2d, 3d from *WFPC2 ISR* 97-08 with this data)
–0.000 => m_{F814W} = 15.353 mag	Contamination correction (0.000 x [49763.4 – 49760.1])
–0.013 => m_I = 15.340 mag	Transformation to Cousins I passband

28.3 Polarimetry

WFPC2 has a polarizer filter which can be used for wide-field polarimetric imaging from about 200 through 700 nm. This filter is a *quad*, meaning that it consists of four panes, each with the polarization angle oriented in a different direction, in steps of 45^o. The panes are aligned with the edges of the pyramid, thus each pane corresponds to a chip. However, because the filters are at some distance from the focal plane, there is significant vignetting and cross-talk at the edges of each chip. The area free from vignetting and cross-talk is about 60" square in each WF chip, and 15" square in the PC. It is also possible to use the polarizer in a partially rotated configuration, which gives additional polarization angles at the expense of more severe vignetting.

Each polarimetry observation consists of several images of the same object with different orientations of the polarizer angle. A minimum of three observations is required to obtain full polarimetry information. This can be achieved by observing the target in different chips, by rotating the filter wheel (partial rotation), or by changing the orientation of the HST field of view in the sky, using a different roll angle. In the latter case, observations must frequently occur at different times, as the solar array constraints on HST allow only a limited range of roll angles at any given time.

Accurate calibration of WFPC2 polarimetric data is rather complex, due to the design of both the polarizer filter and the instrument itself. WFPC2 has an

aluminized pick-off mirror with a 47˚ angle of incidence, which rotates the polarization angle of the incoming light, as well as introducing a spurious polarization of up to 5%. Thus, both the HST roll angle and the polarization angle must be taken into acccount. In addition, the polarizer coating on the filter has significant transmission of the perpendicular component, with a strong wavelength dependence (see Figure 28.1).

Figure 28.1: Parallel and Perpendicular Transmission of the WFPC2 Polarizer

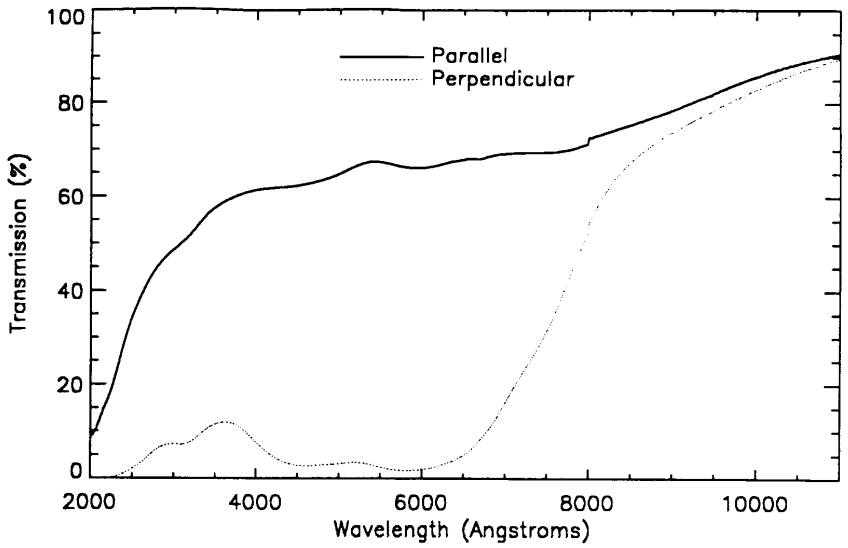

Biretta and McMaster (*WFPC2 ISR* 97-11) recently achieved a calibration accuracy of about 2% rms for well-exposed WFPC2 polarimetry data. Their method uses a Mueller matrix approach to account for the orientation of both telescope and polarizer, the effect of the pick-off mirror, and the significant perpendicular transmission of the polarizer itself. A full description of the motivation behind this approach, the implementation details, and the necessary caveats are given in this document. A web-based tool to aid in the calibration of polarization data has also been developed. With the aid of this tool, polarization properties can be derived for point sources and extended sources from an arbitrary combination of polarized images. The tool is available at:

`http://www.stsci.edu/ftp/instrument_news/WFPC2/Wfpc2_pol/wfpc2-pol2.html`

The procedure to obtain polarization information begins with the calibrated images, as they come out of the pipeline (plus cosmic ray and warm pixel rejection, if appropriate). The characteristics of the polarized images and the fluxes in each image are entered in the Web tool, and the calculation started. The tool then reports the values of the Stokes parameters *I*, *Q*, and *U*, as well as fractional polarization and position angle. The optional **synphot** values in the first part of the tool can be used to fine-tune the results to a specific spectral energy distribution, but are in most cases not necessary.

The tool also reports expressions for *I*, *Q*, and *U* as a function of fluxes in the three images. These can be used to test the sensitivity of the results to errors in the

individual fluxes, or to combine images in order to obtain pixel-by-pixel values of the Stokes parameters for extended objects, resulting in I, Q, and U images.

More details will be provided in a future ISR, as well as in the extensive help available in the web tool itself.

28.4 Astrometry

Astrometry with WFPC2 means primarily *relative* astrometry. The high angular resolution and sensitivity of WFPC2 makes it possible, in principle, to measure precise positions of faint features with respect to other reference points in the WFPC2 field of view. On the other hand, the absolute astrometry that can be obtained from WFPC2 images is limited by the positions of the guide stars, usually known to about 0."5 rms in each coordinate, and by the transformation between the FGS and the WFPC2, which introduces errors of order of 0."1 (see *Instrument Science Report* OSG-006).

Because WFPC2 consists of four physically separate detectors, it is necessary to define a coordinate system that includes all four detectors. For convenience, sky coordinates (right ascension and declination) are often used; in this case, they must be computed and carried to a precision of a few mas, in order to maintain the precision with which the relative positions and scales of the WFPC2 detectors are known. It is important to remember that the coordinates are *not* known with this accuracy. The absolute accuracy of the positions obtained from WFPC2 images is typically 0."5 rms in each coordinate and is limited primarily by the accuracy of the guide star positions.

The recommended way to convert pixel coordinates into relative coordinates is to use the task **metric**, which can handle both WF/PC and WFPC2 images. For WFPC2 images, **metric** corrects for the *geometric distortion* introduced by the camera optics, primarily the field flattening lenses, and brings the four chips into the *metachip* reference system, defined so as to have the same orientation and plate scale as the WF2 chip at its center. These coordinates are then converted into right ascension and declination by using the position and orientation of the WF2 chip. A related task, **invmetric**, can be used to effect the opposite transformation, from right ascension and declination to chip and pixel position. The final relative positions are accurate to better than 0."005 for targets contained on one chip, and 0."1 for targets on different chips. Note that both **metric** and **invmetric** include specialized information about the geometry of WFPC2. They do *not* use the header parameters that describe the world coordinate system (CRVAL1 and 2, CRPIX1 and 2, and the CDMATRIX) to relate positions in different chips. Of these parameters, only the values for WF2 are used to convert the metachip positions to and from right ascension and declination. As a side effect, neither task can work on images that do not contain WF2, for which the **xy2rd** task can be used.

Early WFPC2 images contain header parameters with less accurate values of the plate scale and of the chip-to-chip rotations. The task **uchcoord** will modify

the header parameters of these images to reflect more current information. The task **uchcoord** also corrects the header parameters for an error that occurred between April 11 and 19, 1994. The task will stamp the file after the transformation, to prevent users from unwittingly correcting the same image twice. It is recommended that **uchcoord** be run on all images taken before March 1995; the task will not apply any correction unless it is warranted, and thus it is safe to run on any WFPC2 image. There is also some evidence, both from internal exposures and from a study of many external WFPC2 exposures taken over the years (Ratnatunga et al., 1997), that the relative position of the four detectors may have shifted by up to 0."1 since launch, and especially across the cooldown of April 23, 1994. A regular monitoring program (CAL 7627) is in place to follow such variations. Should they occur again, the relevant tasks, **metric** and **invmetric**, will be modified to return the information appropriate to the date of observation.

Rough coordinates can also be obtained using the task **xy2rd**, which uses the world coordinate system parameters in each group to determine the coordinates associated with a given pixel position. However, **xy2rd** does not use the most recent information on the relative chip positions, and it does not apply the geometric correction. Each can result in an error of about 0."3, especially near the edges of the chip; typical errors are closer to 0."1.

28.5 Dithering

The pixels of the PC undersample the point spread function (PSF) of the HST by a factor of about two, and the pixels of the WF are a factor of two coarser yet. Thus WFPC2 does not recover a substantial fraction of the spatial information that exists at the focal plane of the instrument. However, this information is not completely lost. Some of it can be recovered by *dithering* or *sub-stepping* the position of the chips by non-integral pixel amounts.

The recovery of high frequency spatial information is fundamentally limited by the pixel response function (PRF). The PRF of an ideal CCD with square pixels is simply a square boxcar function the size of the pixel. In practice, the PRF is a function not only of the physical size of the pixels, but also the degree to which photons and electrons are scattered into adjacent pixels, as well as smearing introduced by telescopic position wandering. The image recorded by the CCD is the “true” image (that which would be captured by an ideal detector at the focal plane) convolved with this PRF. Thus, at best, the image will be no sharper than that allowed by an ideal square pixel. In the case of WFPC2, in which at least 20% of the light falling on a given pixel is detected in adjacent pixels, the image is even less sharp.

The PRF of an ideal square pixel, that is a boxcar function, severely suppresses power on scales comparable to the size of the pixel. According to the Shannon-Nyquist theorem of information theory the sampling interval required to capture nearly all of the information passed by square pixels is 1/2 the size *l* of a pixel. This corresponds to dithering the CCD from its starting position of (0,0) to

three other positions, (0,1/2 *l*), (1/2 *l*, 0) and (1/2 *l*, 1/2 *l*); however, in practice, much of the information can be regained by a single dither to (1/2 *l* , 1/2 *l*).

The process of retrieving high-spatial resolution information from dithered images can be thought of as having two stages. The first, reconstruction, removes the effect of sampling and restores the image to that produced by the convolution of the PSF and PRF of the telescope and detector. The more demanding stage, deconvolution (sometimes called restoration), attempts to remove much of the blurring produced by the optics and detector. In effect, deconvolution boosts the relative strength of the high-frequency components of the Fourier spectrum to undo the suppression produced by the PSF and PRF.

If your observations were taken with either of the two dither patterns discussed above, and if the positioning of the telescope was accurate to about a tenth of a pixel (this is usually but not always the case), then you can reconstruct the image merely by interlacing the pixels of the offset images. In the case of a two-fold dither—that is images offset by a vector (n + 1/2, n + 1/2) pixels, where n is an integer—the interlaced images can be put on a square grid rotated 45˚ from the original orientation of the CCD (see Figure 28.2, top). In the case of a four-fold dither, the images are interlaced on a grid twice as fine as the original CCD and coaligned with it (see Figure 28.2, bottom).

Figure 28.2: Interlacing Pixels of Offset Images

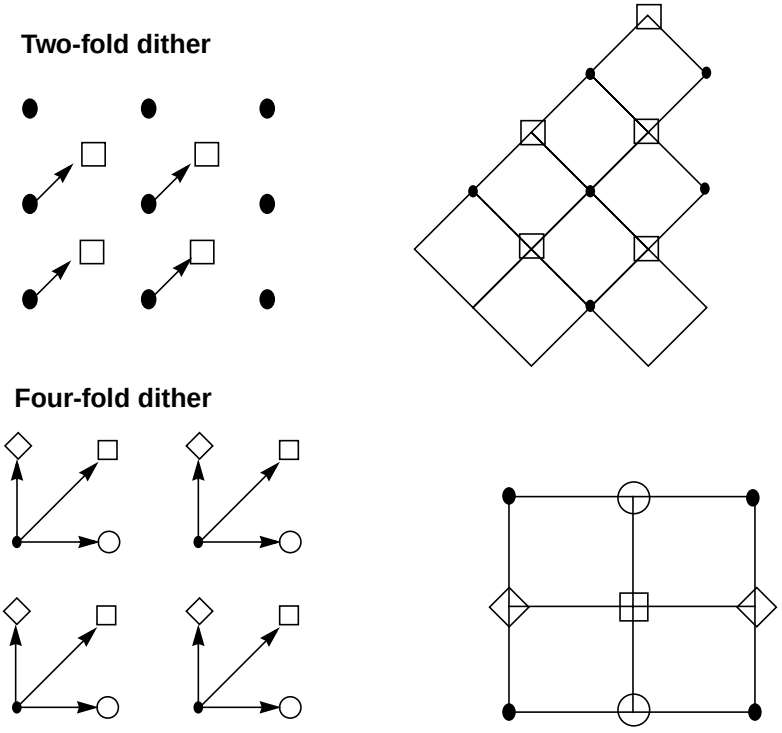

As part of the Hubble Deep Field project, a new method was developed to linearly reconstruct multiple offset images. This method, variable pixel linear reconstruction (also known as *drizzle*), can be thought of as shifting and adding with a variable pixel size. For poorly sampled data, the shifted pixels retain the

initial pixel size—the final image combines the shifts correctly, but the gain in resolution is minimal. For a well-sampled field, such as that of the Hubble Deep Field, the size of the shifted pixels can be made quite small, and the image combination becomes equivalent to interlacing. Drizzling also corrects for the effects of the geometric distortion of WFPC2; correction of geometric distortion is important if shifts between dithered images are of order ten pixels or more.

The drizzle algorithm was implemented as the STSDAS task **drizzle**, as part of the **dither** package, which helps users combine dithered images. The **dither** package is included in STSDAS release v2.0.1 and later, and includes the following tasks:

- **precor**: Determines regions of the image containing astrophysical objects and nulls the remainder of the image, substantially reducing the effect of cosmic rays and chip defects on the offset measurement. The ouput from **precor** is only used for offset determination and not final image creation.
- **offset**: Cross-correlates all four images in a WFPC image, creating output cross-correlation images with names that can be appropriately grouped by later tasks. Uses the task **crossdriz** to perform the cross-correlation.
- **crossdriz**: Cross-correlates two images, after preprocessing which includes trimming, and, if requested, drizzling to remove geometric distortion or rotation. **crossdriz** will also perform a loop over a range of test rotation angles.
- **shiftfind**: Locates the peak in a cross-correlation image and fits for sub-pixel shift information. The search region and details of the fitting can be adjusted by the user.
- **rotfind**: Fits for the rotation angle between two images. **rotfind** is called when **crossdriz** has been used to loop over a range of test rotation angles between two images.
- **avshift**: Determines the shifts between two WFPC2 images by averaging the results obtained on each of the groups after adjusting for the rotation angles between the four groups. **avshift** can also be used to estimate the rotation angle between two different WFPC2 images, when the rotation angle is a small fraction of a degree.
- **blot**: Maps a drizzled image back onto an input image. This is an essential part of the tasks we are developing for removing cosmic rays from singly-dithered images.

Additional information on these tasks is available in Fruchter et al. (1997) and Mutchler and Fruchter (1997), as well as the on-line help files.

Although reconstruction largely removes the effects of sampling on the image, it does not restore the information lost to the smearing of the PSF and PRF. Deconvolution of the images, however, does hold out the possibility of recapturing much of this information. Figure 28.3, supplied by Richard Hook of the ST-ECF, shows the result of applying the Richardson-Lucy deconvolution scheme to HST data, used extensively in the analysis of WF/PC-1 data. The upper-left image shows one of four input images. The upper-right image shows a

deconvolution of all of the data, and the lower two images show deconvolutions of independent subsets of the data. A dramatic gain in resolution is evident.

Figure 28.3: Richardson-Lucy Deconvolution of HST Data

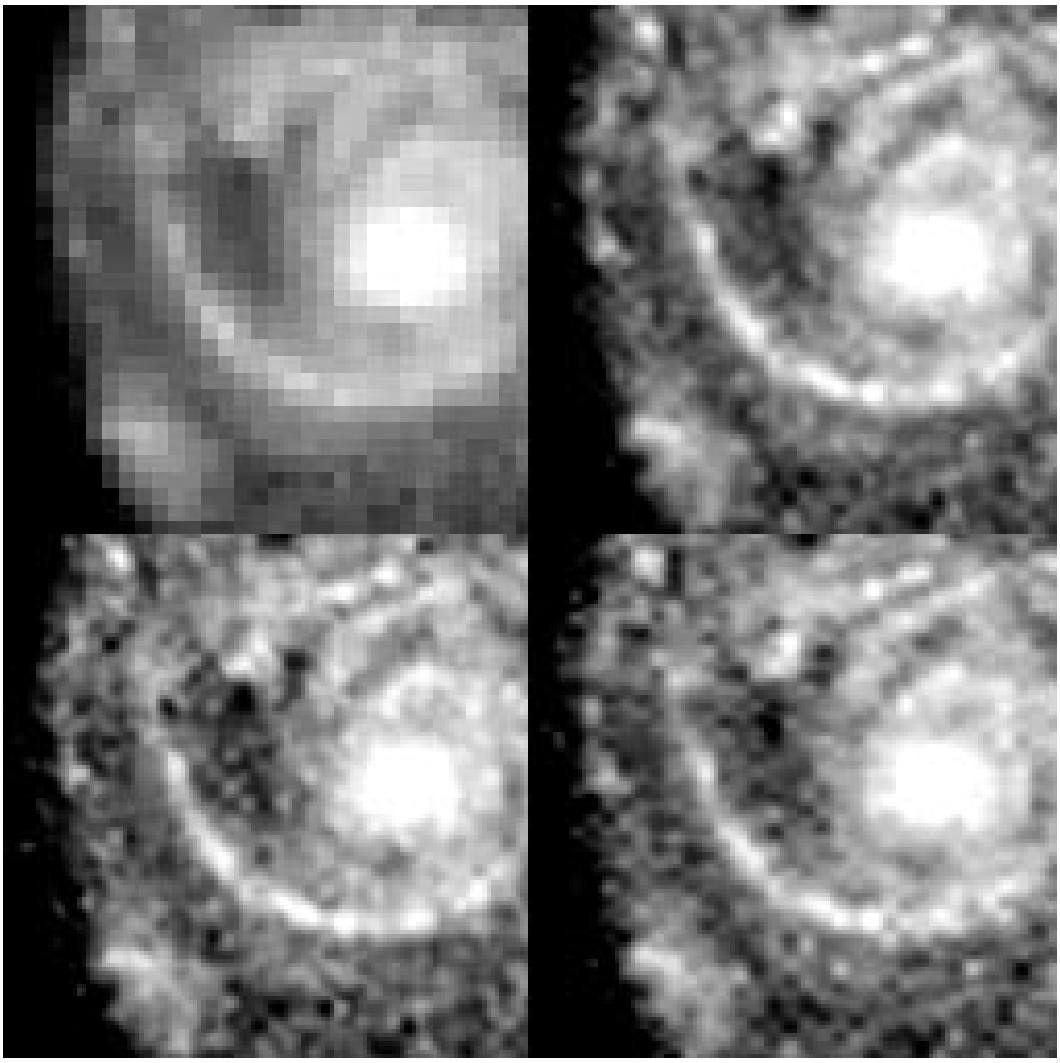

A version of the Richardson-Lucy (RL) deconvolution scheme capable of handling dithered WFPC2 data is already available to STSDAS users. It is the task **acoadd** in the package **stsdas.contrib**. In order to use **acoadd**, users will need to supply the program both with a PSF (which in practice should be the convolution of the PRF with the optical PSF) and with the offsets in position between the various images. The position offset between the two images can be obtained using the task **crossdriz** in the **dither** package.

In principle, image deconvolution requires an accurate knowledge of both the instrument PSF and PRF. At present, our best models of the WFPC2 PSF come from the publicly available TinyTim software (Krist, 1995). The quality of the TinyTim model can be improved substantially by taking into account the exact position of the source within the pixel. Remy et al. (1997) discuss how this can be

accomplished by generating multiple TinyTim images at various focus and jitter values, oversampled with respect to the camera pixels. At present, this is very labor-intensive, and the results cannot be easily integrated into the existing deconvolution software. Another limitation of the existing software is that it cannot incorporate the significant variation of the PSF across the field of view. As a result, the Richardson-Lucy approach can only be applied to limited regions of a chip at a time. Nonetheless, tests done on WFPC2 images suggest that RL deconvolution can give the WFPC2 user a substantial gain in resolution even in the presence of typical PSF and PRF errors. Users interested in more information on dithering, reconstruction, and deconvolution should consult the February and September 1995 issues of the ST-ECF Newsletter, where these issues are discussed in detail.

28.6 Accuracy of WFPC2 Results

Table 28.6 summarizes the accuracy to be expected from WFPC2 observations in several areas. The numbers in the table should be used with care, and only after reading the relevant sections of this handbook and the documents referenced therein; they are presented in tabular form here for easy reference.

Table 28.6: Accuracy Expected in WFPC2 Observations

Procedure	Estimated Accuracy	Notes
	Calibration (flatfielding, bias subtraction, dark correction)	
Bias subtraction	0.1 DN rms	Unless bias jump is present
Dark subtraction	0.1 DN/hr rms	Error larger for warm pixels; absolute error uncertain because of dark glow
Flatfielding	<1% rms large scale	Visible, near UV
	0.3% rms small scale	
	~10%	F160BW; uncertain
	Relative photometry	
Residuals in CTE correction	< 1% rms (above 1000 DN)	
	3% rms (at 100 DN)	
Long vs. short anomaly (uncorrected)	< 1% rms (above 10000 DN)	
	5% (at 1000 DN)	
	15% (at 100 DN)	
Aperture correction	4% rms focus dependence (1 pixel aperture)	Can (should) be determined from data
	<1% focus dependence (> 5 pixel)	
	1-2% field dependence (1 pixel aperture)	
Contamination correction	3% rms max (28 days after decon) (F160BW)	
	1% rms max (28 days after decon) (filters bluer than F555W)	
Background determination	0.1 DN/pixel (background > 10 DN/pixel)	May be difficult to exceed, regardless of image S/N
Pixel centering	< 1%	
	Absolute photometry	
Sensitivity	< 2% rms for standard photometric filters	Red leaks are uncertain by ~10%
	2% rms for broad and intermediate filters in visible	
	< 5% rms for narrow-band filters in visible	
	2-8% rms for UV filters	
	Astrometry	
Relative	0.005" rms (after geometric correction)	Same chip
	0.1" (estimated)	Across chips
Absolute	1" rms (estimated)	

28.7 References

- Casertano, S., 1998, in *The 1997 HST Calibration Workshop*, eds. S. Casertano et al., (Baltimore: Space Telescope Science Institute), in press.
- Fruchter, A.S., et al., in *The 1997 HST Calibration Workshop*, eds. S. Casertano et al., (Baltimore: Space Telescope Science Institute), in press.
- Harris, H.C., et al., 1993, *AJ*, 105, 1196.
- Holtzman, J.A., et al., 1995a, *PASP*, 107, 156.
- Holtzman, J.A., et al., 1995b, *PASP*, 107, 1065.
- Krist, J., 1995, "Simulation of HST PSF Using TinyTim," in *Astronomical Data Analysis, Software, and Systems IV*, Shaw et al., eds. (San Francisco: Astronomical Society of the Pacific), p. 349.
- Mutchler, M., and A. Fruchter, 1998, in *The 1997 HST Calibration Workshop*, eds. S. Casertano et al., (Baltimore: Space Telescope Science Institute), in press.
- Oke, J.B., 1974, *ApJS*, 27, 21.
- Ratnatunga, K.U., et al., 1998, in *The 1997 HST Calibration Workshop*, eds. S. Casertano et al., (Baltimore: Space Telescope Science Institute), in press.
- Remy, M., et al., 1998, in *The 1997 HST Calibration Workshop*, eds. S. Casertano et al., (Baltimore: Space Telescope Science Institute), in press.
- Surdej, J., et al., 1998, in *The 1997 HST Calibration Workshop*, eds. S. Casertano et al., (Baltimore: Space Telescope Science Institute), in press.
- Trauger, J.T., et al., 1994, *ApJ*, 435, L3.
- Trauger, J.T., 1998, in *The 1997 HST Calibration Workshop*, eds. S. Casertano et al., (Baltimore: Space Telescope Science Institute), in press.
- Wiggs, M.S., et al., 1998, in *The 1997 HST Calibration Workshop*, eds. S. Casertano et al., (Baltimore: Space Telescope Science Institute), in press.